Solution-Processed Functional Zinc Oxide Films

Jeongsoo Hong*, Kenichi Katsumata**, Yunzi Xin***, Takashi Shirai***, Nobuhiro Matsushita****

*Department of Electrical Engineering, Gachon University, Korea
1342 Seongnamdaero, Sujeong-gu, Seongnami-si, Gyeonggi-do, KOREA

**Photocatalysis International Research Center, Tokyo University of Science, Japan
2641 Yamazaki, Noda-shi, Chiba-ken 278-8510, JAPAN

***Advanced Ceramics Research Center, Nagoya Institute of Technology, Japan
Gokiso-cho, Showa-ku, Nagoya, Aichi 466-8555, JAPAN

****Department of Materials Science and Engineering, Tokyo Institute of Technology, Japan
2-12-1 Ookayama, Meguro-ku, Tokyo 152-8550, JAPAN

ZnO is promising Functional material to apply to various electronic devices, and aqueous solution process named spin-spray method which used in this study is the simplest and cost effective method for fabricating ZnO films. In this paper, we fabricated ZnO films with various surface morphologies and investigated the functional properties of solution-processed ZnO film.

Keywords: ZnO, Spin-spray, Photocatalysis, Conductivity, Thin film

1. Introduction

In recent years, photo-functional ceramic materials have great applied potential for electronic and photocatalytic applications [1, 2]. Among the various ceramic materials, zinc oxide (ZnO) is one of the semiconductor materials having large exciton binding energy (~ 60 meV) with wide gap energy, and these basic properties can lead to blue and ultra-violet optical devices. In addition, ZnO is well-known photocatalytic material, and it has been intensively studied for application of photocatalysis [3]. Additionally, ZnO can be fabricated with various structures such as rods, tubes, flowers and tetrapods, it means that ZnO film can be applied to various application fields [4-6].

In case of the application of electronic device, ZnO film deposited by vacuum process such as sputtering is widely used as a transparent electrode and channel layer due to their high crystallinity, transparency and electrical conductivity. [7-9] However, it requires high cost vacuum equipment, because of this, many researchers are focusing on solution process as an alternative fabrication method. ZnO film fabricated by solution process has various kinds of surface morphologies. In addition, these variation of surface morphologies affect to specific surface area, and it is one of the factors for decide the photocatalytic performance. [10]

However, ZnO film which fabricated by solution process such as sol-gel, and hydrothermal method, contains the large amount of organic substances in the film, it resulted degradation of electrical conductivity. [11] For this reason, post-annealing process at high temperature is used for improvement of the electrical conductivity, after deposition of film. [12, 13] However, it causes the change of crystallographic property, and this process is difficult to apply for flexible electronic device which used plastic substrates. [14, 15]

This problem can be solved by photocatalytic reaction of ZnO. As mentioned before, ZnO has photocatalytic property, and photocatalytic reaction of ZnO can be occurred under ultraviolet (UV) irradiation. Organic substance in the film can be decomposed by photocatalytic reaction of ZnO without annealing process, and change of crystallographic property, for this reason, it is expected to bring positive effects to electrical conductivity.

In this study, we fabricated ZnO films having various surface morphology, and tried to graft the photocatalytic reaction on electronic application, and evaluated the photocatalytic performance.

First, we fabricated the ZnO films having various surface morphologies such as rod, dense, and flower-like structure by aqueous solution process named spin-spray method. And then, as-fabricated ZnO films were subjected to UV irradiation for improvement of electrical conductivity. In addition, we investigated effect of surface morphology on photo-degradation of rhodamine

B, and the relationship between improved electrical conductivity by photocatalytic reaction of ZnO film and hydrogen production.

2. Experimental Procedure

2.1 Spin-spray method

There are various solution processes used to fabricate ZnO films such as chemical bath deposition, hydrothermal treatment, spray pyrolysis and the sol-gel method. However, these methods have some disadvantages such as requiring a seed layer for good adhesion and annealing at high temperature (>300° C) to improve the crystallinity. Seed layers are inefficient because they are generally deposited by sputtering. Deposition of a seed layer by solution processes such as spin-coating involves repeated deposition-annealing cycles to attain the required thickness. Additionally, annealing ZnO films at high temperature is unsuitable for flexible application. Therefore, a novel solution process that can directly deposit a crystalline film without a seed layer or annealing is required.

In this study, ZnO films were deposited by a spin-spray process using aqueous solution (Figure 1). This process is environmentally friendly, simple and has a high deposition rate (>100 nm/min). Furthermore, this spin-spray method can deposit high-quality crystalline films at low substrate temperature (<100° C) without the need for a seed layer or annealing.

2.2 Fabrication of ZnO films

The glass substrates were first ultrasonically cleaned in deionized water and ethanol for 10 min to remove impurities on the substrate surface. Then, the substrates were exposed to discharge plasma for 10 min to increase the hydrophilicity of their surfaces.

To deposit the ZnO films having rod and dense structures, the source solution was prepared by dissolving $Zn(NO_3)_2{\cdot}6H_2O$ in Millipore deionized water to give a concentration of $Zn(NO_3)_2{\cdot}6H_2O$ of 10 mmol. The reaction solution was prepared by dissolving 120 mL of NH_3 solution in Millipore deionized water. Sodium citrate was added to the reaction solution to give concentrations of 0 and 2 mmol. NH_3 solution was used as a pH adjuster and sodium citrate was used as a surfactant to fabricate ZnO films with a continuous structure [30]. The source and reaction solutions were simultaneously and continuously sprayed onto the rotating substrates for 10 min at 90° C.

In case of the flower-like ZnO film, source solution

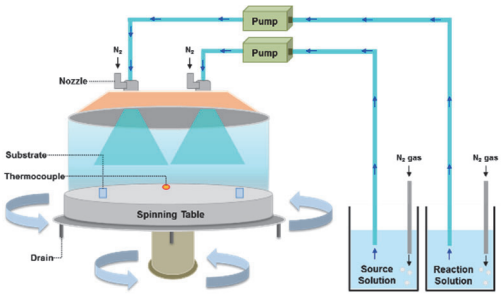

Figure 1 Illustration of spin-spray method.

including $Zn(NO_3)_2{\cdot}6H_2O$ and reaction solution including NaOH (4-40 mM, as a pH adjuster, without additive) were used for deposition of film at 90° C for 10 min.

2.3 Evaluation of ZnO film

The conductivity and transmittance of the films were evaluated by a Hall Effect measurement system (HL5500, Nanometrics) and UV-Vis spectrometer (Lambda 35 spectrometer, Perkin Elmer), respectively. Surface and cross-sectional morphology were observed by SEM (S4000, Hitachi, Japan). Structural properties were analyzed by XRD (Rint2000, Rigaku) with CuKα radiation (λ =1.5418 Å). Changes in chemical states were investigated by XPS (ESCA-3200, Shimadzu Corp.).

All films were were subjected to UV irradiation by using Black-Light-Blue (BLB) lamp (Intensity = 0.8 mW/cm^2) and 200 W Hg-Xe UV lamp, 2.5 mW/cm^2) for evaluation of photocatalytic performance of ZnO film. Existence of organic substance in the as-fabricated ZnO films were confirmed by Fourier transformed infrared (FT-IR) measurements (JIR-7000, JEOL). Generated CO_2 and H_2 gas was detected by gas chromatography (GC-2014F, Shimadzu).

3. Result and discussion

3.1 Surface structures of ZnO film

Figure 2 shows the XRD patterns and surface morphologies of all samples. As-fabricated ZnO films indicated rod, dense, and flower-like structures, their surface structures were changed by solution conditions. First, as-fabricated ZnO film without surfactant indicated rod structure (S1), however, it changed to dense surface morphology (S2) by adding citrate. ZnO film having rod structure oriented along the c-axis, however, preferential orientation was changed from (002) to (101), it might be a reason for varied surface morphology [16-17]. In addition, flower-like ZnO film was fabricated using NaOH without additive. Expected

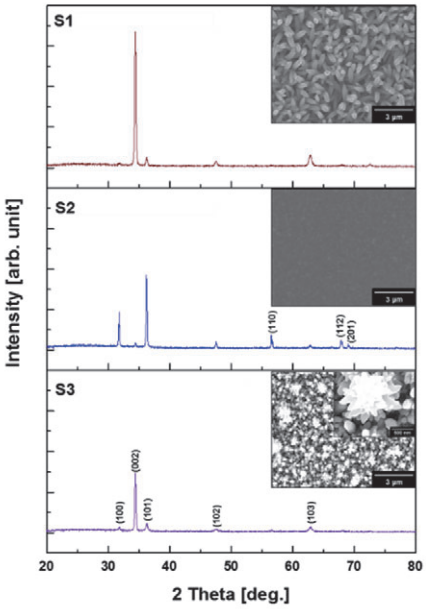

Figure 2 XRD patterns and surface morphologies of as-fabricated ZnO films.

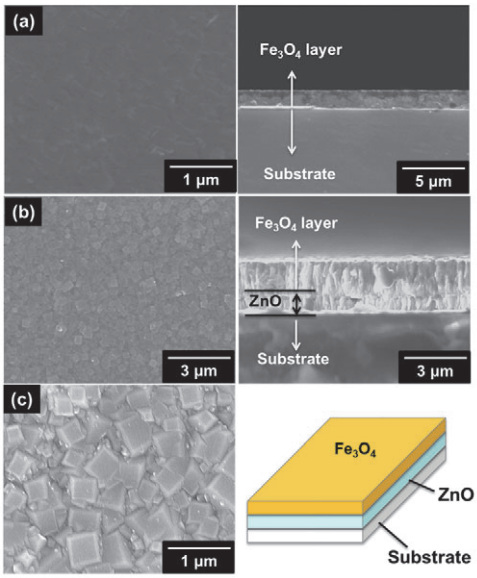

Figure 3 SEM images of as-fabricated Fe_3O_4 (a), Fe_3O_4/ZnO (b, C) films.

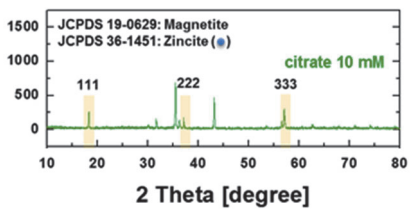

Figure 4 XRD patterns of Fe_3O_4/ZnO films.

ZnO growth reaction by using NaOH as a pH adjuster is as follow process,

$$Zn^{2+} + 2OH^- \rightarrow Zn(OH)_{2(aq)} \rightarrow ZnO_{(s)} + H2O$$

$$Zn(OH)_{2(aq)} + 2H_2O \rightarrow Zn(OH)_4^{2-} + 2H^+ \rightarrow ZnO_{(s)} + 3H_2O$$

Successively applied large amount of OH^- ions with increase of NaOH concentration affect to formation of growth sites on the pre-existing rod surface, and ZnO grew as a single crystal on this growth sites. As a result, as-fabricated ZnO film exhibited flower- like structure due to increase of amount of small-sized nanorods on pre-existing rod surface [18].

3.2 Heterostructured Fe_3O_4 / ZnO Film

The magnetite (Fe_3O_4) has been drawing attention for spintronic devices due to its relatively high Curie temperature among the half-metallic materials. In addition, the epitaxial growth of Fe_3O_4 film based on metallic or semiconductor films are important for tunneling magnetoresistive and giant magnetoresistive devices as a polarized spin injector [19]. To apply for these applications, various kinds of materials such as ZnO is considered as a metallic under layer for fabricating heterostructured double-layered films of Fe_3O_4/ semiconductor film.

Figure 3 shows SEM images of Fe_3O_4 single layer and heterostructured Fe_3O_4/ZnO films. Surface morphologies, they were changed by ZnO single layer which deposited with different citrate concentrations [20]. Especially, Fe_3O_4 /ZnO fabricated on as-deposited ZnO layer at citrate concentration of 10 mM, it had cubic shape, as shown in Figure 3-(c). To confirm the more details of crystallographic properties, heterostructured Fe_3O_4/ZnO films were analyzed by XRD.

Figure 4 shows the XRD patterns of hetero-structured Fe_3O_4/ZnO films fabricated on as-deposited ZnO layer. All diffraction peaks were identified as ZnO and magnetite phase and another impurity peaks were not detected.

In addition, although their peaks intensities were weak, preferential orientation along the (nnn) plane such as (111), (222), and (333) peaks were observed at 18.3, 37.1, and 57.0°. Generally, these preferential orientations along the (nnn) plane are observed in Fe_3O_4 layer deposited on ZnO (00n) layer deposited by dry process such as sputtering [21].

However, heterostructured Fe_3O_4/ZnO films having preferential orientations along the (nnn) planes were simply obtained by solution process at low substrate

temperature without post-annealing process. It suggests that solution process can be also one of the possible ways to fabricate the polarized spin injector which strict orientation control is required.

3.3 Electrical conductivity of ZnO film

A widely used method to improve conductivity is increasing the carrier concentration by metal ion doping, often with group III dopants such as In, Al, and Ga [22-25]. These dopants substitute Zn ions and generate free electrons, causing the carrier concentration of ZnO to increase. However, in the case of solution-processed metal ion-doped ZnO films, hydroxide and/or layered double hydroxides are formed in the solution or on the film surface, which lead to decreased conductivity [26]. Another method to improve the conductivity of ZnO is to increase its mobility by thermal treatment using a suitable temperature, time and atmosphere [27-30]. Crystallographic properties such as crystallinity and crystallite size strongly affect mobility and thus conductivity [31]. However, conventional thermal treatment processes generally use high temperature and/or long treatment time, resulting in negative side effects such as films peeling off the substrate because of defect formation and stress [32], and oxygen deficiency in the films. Oxygen deficiency can degrade electrical conductivity because of photon scattering [23, 33].

In this study, ZnO film having dense structure is fabricated by a spin-spray method using aqueous solutions followed by thermal treatment under different

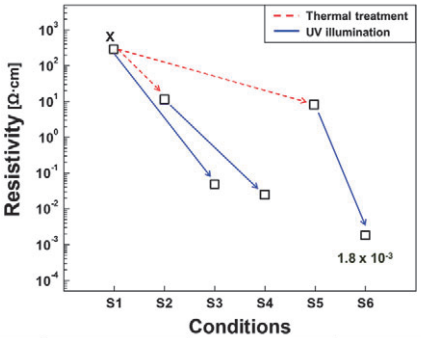

	Thermal treatment	UV illumination	etc.
S1	-	-	as-deposited
S2	100°C, Air	-	-
S3	-	BLB lamp, 24 h	-
S4	100°C, Air	BLB lamp, 24 h	-
S5	100°C, H_2 3%	-	-
S6	100°C, H_2 3%	BLB lamp, 24 h	-

Figure 5 Dependence of resistivity on thermal treatment and UV irradiation.

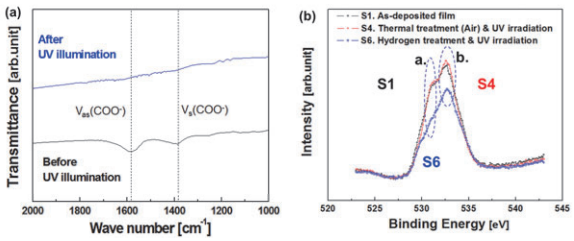

Figure 6 FT-IR spectra and change of XPS O1s peaks of ZnO films.

atmospheres and/or UV irradiation. The ZnO films treated by both hydrogen reduction and UV irradiation exhibits high conductivity because of their high mobility and high carrier concentration.

As-deposited ZnO film having dense structure, indicated high resistivity, before UV irradiation, as shown in Figure 5. However, resistivity was gradually decreased as UV irradiation time passes, as a result, resistivity of UV irradiated film decrease to ~10^{-2} Ω·cm, after UV irradiation for 24 h (S3). As a reason for this result, we assumed that increase of carrier concentration occurred from decomposition of organic substance caused by photocatalytic activity of ZnO, attribute to decrease in resistivity [32]. As shown in Figure 6-(a) (FT-IR spectra), two peaks of carboxyl group originating from citrates were observed, it means as-deposited film contains organic substance. While these peaks disappeared after UV irradiation for 24 h, from that result, we could confirm the decomposition of organic

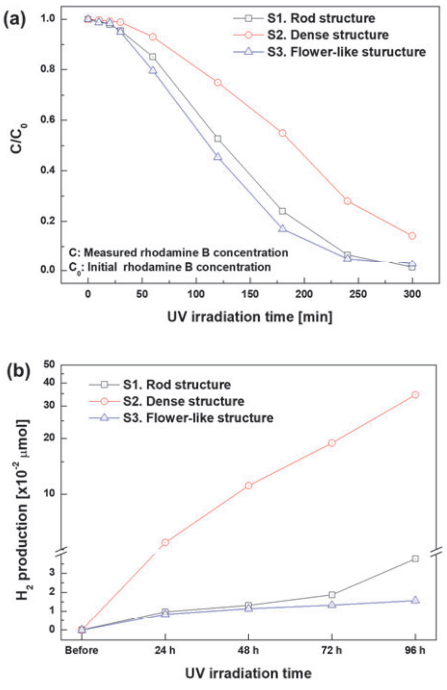

Figure 7 Photo-dgradation of rhodamine B and hydrogen production of as-fabricated ZnO films, under UV irradiation.

substance in the film. From the result, we thought that photocatalytic activity of ZnO might be contribute to decrease of resistivity. ZnO is one of the photocatalytic materials, and it reacts photocatalytic reaction, under UV irradiation. By photocatalytic reaction of ZnO, organic substances such as carboxyl group in the film were decomposed. It leads to photo-induced doping of C and/or H into the ZnO, and resulted in generating the electron. [22, 32, 33] Generated electrons play a role as a shallow-donors, it would attribute to increase of carrier concentration (~10^{20} cm^{-3}). [33]

Another reason for the improved conductivity of the ZnO films is following thermal treatment in hydrogen atmosphere. The conductivity of ZnO films is affected by surface defects, negatively charged oxygen species and/or organic impurities [34-36]. Negatively charged oxygen species form depletion regions at grain boundaries and act as trapping sites [35], which has negative effects on both electron mobility and conductivity. Thermal treatment with hydrogen is a simple and effective method to improve mobility because hydrogen readily removes negatively charged oxygen species.

Comparing S4 and S6 reveals that hydrogen reduction effectively improved mobility; the mobility of S6 (11.2 $cm^2V^{-1}s^{-1}$) was about ten times higher than that of S4 (1.2 $cm^2V^{-1}s^{-1}$). This high mobility also contributed to the low resistivity of S6 of $1.8\times10^{-3}\Omega\cdot$ cm. During hydrogen reduction, negatively charged oxygen species are desorbed from grain boundaries so that the potential barrier is lowered [36]. Additionally, hydrogen passivates the grain boundary surface to remove organic materials and negatively charged oxygen species [37]. To confirm that hydrogen reduction increases mobility, S1, S4, and S6 were analyzed by XPS.

The O1s spectra for S1, S4 and S6 are presented in Figure 6-(b). Two peaks at 530.2 and 532.5 eV were observed by fitting with a Lorentzian distribution. The peak at 530.2 eV (a) is assigned O^{2-} ions surrounded by Zn atoms in the wurtzite-structured ZnO, while that at 532.5 eV (b) is attributed to loosely bound oxygen species such as CO_3, O_2, H_2O and carboxyl groups on the ZnO surface and/or grain boundaries [38-41]. Here, loosely bound oxygen species generated by negatively charged oxygen might deteriorate film mobility by hindering electron transfer and trapping free electrons. The O1s signals of S1 and S4 were similar. In contrast, the peak at 532.5 eV for S6 was of lower intensity than those of S1 and S4.

This corresponds to a reduction in the amount of negatively charged oxygen species on the ZnO surface and/or grain boundaries in S6 compared with those in S1 and S4. As mentioned above, this would lead to a decrease in potential barrier, causing the mobility of the hydrogen-treated ZnO film to increase. Additionally, a marked decrease in the intensity of the peak at 530.2 eV was also observed for S6 compared with those of S1 and S4. This means the number of O^{2-} ions surrounded by Zn atoms in the wurtzite-structured ZnO was decreased in S6, so the number of oxygen vacancies was increased, which also improved mobility.

3.4 Photocatalytic performance of ZnO film

The performance of degradation is affected by reaction conditions such as pH in solution, light intensity, and additives. [42] However, in this study, we fixed the reaction conditions to investigate the influence of surface morphology on photo-degradation property. As shown in Figure 7-(a), degradation rates of each samples were different, and all samples completely decomposed the rhodamine B, except densely structured ZnO film. Reason for different degradation rate might be related with specific surface area. Rod, and flower-like structure have high specific surface area than dense structure. That means they can adsorb more rhodamine B in their surface than dense structure, it would be affected to photo-degradation of rhodamine B.

Photocatalytic performance of ZnO film was investigated through the hydrogen production, as shown in Figure 7-(b). Evaluation of hydrogen production accomplished with using 5 vol% aqueous methanol solution of 20 ml, under UV light (200 W Hg-Xe lamp, 2.5 mW/cm^2). All films produced the hydrogen, however, amount of produced hydrogen gas shows clear distinction. First, we anticipated that ZnO films having rod and flower-like structure produce larger amount of hydrogen gas than densely structured ZnO film. Because, we already confirmed that high specific surface area accelerates the photocatalytic activity, from the result of photo-degradation performance. However, densely structured ZnO film indicated the higher hydrogen production rate than the other samples, because of this, we attention to the correlation between conductivity of ZnO film and high hydrogen production capability, as a reason for result.

Decomposition of organic substance is playing an important role not only conductivity, but also it affects

to hydrogen production. Mentioned above, densely structured ZnO film contains the organic substance which induced from additive (citrate), however they are decomposed by photocatalytic reaction of ZnO, under UV irradiation.

Decomposed organic substance generates electrons by photo-induced doping, and they play a role as a shallow donor. These electrons cause the activation of intermediate band gap between valence band and conduction band and it leads to increase in amount of positively-charged hole and electron generating under UV irradiation. [43] As a result, large amount of H^+ and OH radical are produced from water, it could be one of the reason for high hydrogen production rate.

Another possible reason is surface defect such as oxygen vacancy. As mentioned, we confirmed the generation of CO_2 from the ZnO film, during UV irradiation (Figure 8). It means oxygen which placed in surface and/or the inside of the film is desorbed by decomposition of organic substance and the resulting oxygen vacancy trap the electron and hole, respectively. It prevents the recombination with electron and holes, as a result, amount of hydrogen production is increased.

4. Conclusion

In this study, we fabricated ZnO films having rod, dense, and flower-like structure using aqueous solution process and investigated their functional properties.

Heterostructured Fe_3O_4/ZnO film was fabricated by successional deposition of Fe_3O_4 layer on ZnO layer. They indicated the preferential orientation along the (nnn) plane, while other peaks which identified Fe_3O_4 were also confirmed. The SEM images for as-fabricated Fe_3O_4/ZnO film revealed that the formed crystallites in Fe_3O_4 layer had cubic phase.

In case of the conductivity, the lowest resistivity of 1.8 $\times 10^{-3}$ Ω·cm with a mobility of 11.2 $cm^2V^{-1}s^{-1}$ and carrier concentration of ~10^{20} cm^{-3} was achieved by hydrogen reduction and UV irradiation.

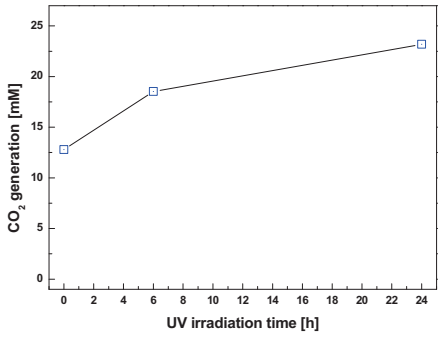

Figure 8 Generation of CO_2, during UV irradiation,

Photo-degradation of rhodamine B solution was observed from the all samples and degradation rate was affected by their surface morphology.

All films produced hydrogen gas from the aqueous methanol solution, and high-conductivity ZnO film having dense structure generated the most amount of hydrogen gas, under UV light.

Reference

[1] U. Ozgur, D. Hofstetter, and H. Morkoc, Proceedings of IEEE, 98 (2010) 1255.

[2] T. Xu, L. Zhang, H. Cheng, and Y. Zhu, Appl. Catal. B: Environ. 101 (2010) 387.

[3] V. A. Coleman and C. Jagadish, Zinc Oxide Bulk, Thin Films and Nanostructures, 2006 Elsevier Limited.

[4] Boris I. Kharisov, Recent Partents on Nanotechnology, 2 (2008) 190.

[5] D. Chu, Y. Masuda, T. Ohji, and K. Kato, J. Am. Ceram. Soc. 93 (2010) 887.

[6] Y. Fang, X. Wen, S. Yang, Q. Pang, L. Ding, J. Wang, and W. Ge, J. Sol-Gel Tech. 36 (2005) 227.

[7] J. Hong, N. Matsushita, and K. Kim, Semicond. Sci. Tech. 29 (2014) 075007 (5pp).

[8] Y. Kawamura, M. Horita, Y. Ishikawa, and Y. Uraoka, J. Dis. Tech. 9 (2013) 694.

[9] L. Chen, W. Chen, J. Wang, and F. C. Hong, Appl. Phys. Lett. 85 (2004) 5630.

[10] H. Cheng, J. Wang, Y. Zhao, and X. Han, RSC Adv. 4 (2014) 47031.

[11] J. Hong, K. Katsumata, and N. Matsushita, J. Electron. Mater. 45 (2016) 4875.

[12] N. Sadananda Kumar, Kasturi V. Bangera, and G. K. Shivakumar, Appl. Nanosci. 4 (2014) 209.

[13] A. Wang, T. Chen, S. Lu, Z. Wu, Y. Li, H. Chen, and Y. Wang, Nanoscale Res. Lett. 10 (2015) 75 (10pp).

[14] J. Hong, H. Wagata, K. Katsumata, and N. Matsushita, Mater. Sci. Semicond. Process. 47 (2016) 20.

[15] Y. Lin, C. Hsu, M. Tseng, J. Shyue, and F. Tsai, ACS Appl. Mater. Interfaces 7 (2015) 22610.

[16] H. Wagata, N. Ohashi, T. Taniguchi, A. K. Subramani, K. Katsumata, K. Okada, N. Matsushita, Cryst. Growth Des. 10 (2010) 3502.

[17] J. Hong, H. Wagata, N. Ohashi, K. Katsumata, K. Okada, N. Matsushita, J. Electron. Mater. 44 (2015) 2657.

[18] J. Hong, N. Matsushita, T. Shirai, K. Nakata, C. Terashima, A. Fujishima, K. Katsumata, Chem. Asian J. 12 (2017) 2480.

[19] F. Qin, Y. Naozaki, and K. Matsuyama, J. Mag. Mag.

Mater. 272 (2004) e1835.
[20] J. Hong, K. Katsumata, and N. Matsushita, IEEE Trans. Mag. 99 (2015) 1.
[21] K. S. Yoon, J. H. Koo, Y. H. Do, K. W. Kim, C. O. Kim, and J. P. Hong, J. Mag. Mag. Mater. 285 (2004) 125.
[22] R. C. Hoffmann, M. Kaloumenos, S. Heinschke, E. Erdem, P. Jakes, R.A. Eichel, and J.J. Schneider, J. Mater. Chem. C 1 (2013) 2577.
[23] J. Hong, N. Matsushita, and K.H. Kim, Thin Solid Films 531 (2013) 238-242.
[24] T. T. T. Vo, Y. H. Ho, and P. H. Lin, Cryst. Eng. Comm. 15 (2013) 6695.
[25] A. Z. Barasheed, S. R. Sarath Kumar, and H. N. Alshareef, J. Mater. Chem. C 1 (2013) 4122.
[26] E. Hosono, S. Fujihara, and T. Kimura, J. Mater. Chem. 14 (2004) 881.
[27] Z. Lin, J. Chang, C. Jiang, J. Zhang, J. Wu, and C. Zhu, RSC Adv. 4 (2014) 6646.
[28] D. Raoufi, and T. Raoufi, Appl. Surf. Sci. 255 (2009) 5812.
[29] K. Laurent, D.P. Yu, S. Tusseau-Nenez, and Y. Leprince-Wang, J. Phys. D: Appl. Phys. 41 (2008) 195410.
[30] F. Ruske, M. Roczen, K. Lee, M. Wimmer, S. Gall, J. Hupkes, D. Hrunski, and B. Rech, J. Appl. Phys. 107 (2010) 013708.
[31] X. Yan, Z. Li, R. Chen, and W. Gao, Cryst. Growth Des. 8 (2008) 2406.
[32] B. P. Shantheyanda, V. O. Todi, and K. B. Sundaram, J. Vac. Sci. Technol. A 29 (2011) 051514.
[33] Y. S. Jung, J. Y. Seo, D. W. Lee, and D. Y. Jeon, Thin Solid Films 445 (2003) 63.
[34] A. Kushwaha, and M. Aslam, J. Phys. D: Appl. Phys. 46 (2013) 4851040.
[35] Z. G. Wang, X. T. Zu, S. Zhu, and L. M. Wang, Physica E 35 (2006) 199.
[36] H. J. Jin, Y. H. Jeong, and C. B. Park, Trans. Elec. Electron. Mater. 9 (2008) 67.
[37] N. H. Nickel, N. M. Johnson, and W. B. Jackson, Appl. Phys. Lett. 62 (1993) 3285.
[38] H. Wagata, N. Ohashi, K. Katsumata, H. Segawa, Y. Wada, H. Yoshikawa, S. Ueda, K. Okada, and N. Matsushita, J. Mater. Chem. 22 (2012) 20706.
[39] H. J. Bong, W. H. Lee, D. Y. Lee, B. J. Kim, J. H. Cho, and K. W Cho, Appl. Phys. Lett. 96 (2010) 192115.
[40] T. Ohsawa, Y. Adachi, I. Sakaguchi, K. Matsumoto, H. Haneda, S. Ueda, H. Yoshikawa, K. Kobayashi, and N. Ohashi, Chem. Mater. 21 (2009) 144.
[41] H. Wagata, N. Ohashi, T. Taniguchi, A.K. Subramani, K. Katsumata, K. Okada, and N. Matsushita, Cryst. Growth Des. 10 (2010) 3502.
[42] R. Chen, X. Zhang, H. Liu, X. Song, and Y. Wei, RSC adv. 5 (2015) 76548.
[43] P. Zhang, R. Y. Hong, Q. Chen, and W. G. Feng, Powder Tech. 253 (2014) 360.